Z. Dt. Ges. Geowiss. (J. Appl. Reg. Geol.), **172 (3)**, p. 365–379, 7 figs., 3 tables
Published online November 2021

Article
Open Access

Quantifying model uncertainty of a geothermal 3D model of the Cenozoic deposits in the northern Upper Rhine Graben, Germany

Jeroen van der Vaart[1], Kristian Bär[1], Matthis Frey[1], John Reinecker[2] & Ingo Sass[1,3,4*]

Van der Vaart, J., Bär, K., Frey, M., Reinecker, J. & Sass, I. (2021): Quantifying model uncertainty of a geothermal 3D model of the Cenozoic deposits in the northern Upper Rhine Graben, Germany. – Z. Dt. Ges. Geowiss., 172: 365–379, Stuttgart.

Abstract: This study presents the advantages of quantifying the model uncertainty for the example of the northern Upper Rhine Graben, a region known for its high geothermal potential in central Europe and its complex structural setting. In geothermal exploration, geological models are often taken as a nearly true representation of the actual subsurface. The public available models created of the northern Upper Rhine Graben are no exception to this reception. While these projects give a great insight into the geological structure, the lack of quantified uncertainty mapping limits practical use for engineering purposes. The limitation comes from the lack of quantitative knowledge, conveyed in the provided qualitative uncertainty ranges. Without a proper understanding of these ranges, exploration risks cannot be properly assessed.

This study explores the sources and impact of errors that lay ground to the structural uncertainty within a geothermal model in the northern Upper Rhine Graben. Error ranges of input data are used to establish probability distribution functions. With a custom-made stochastic workflow, using Monte Carlo simulation, maps of uncertainty are created for several formations and groups, indicating extent of uncertainty for their horizons. Furthermore, using several different sources of errors, the effects of uncertainty reduction by additional seismic and well data acquisition are explored.

Keywords: Uncertainty modelling, northern Upper Rhine Graben, geothermal exploration, exploration risk, probability of success

1. Introduction

As man-made climate change results in a global temperature increase, high investments are needed for the fast implementation of renewable energy sources to cover the increasing energy demands. To remedy the CO_2 output significantly, a mixture of renewable energy generation technologies and a fast transition towards it is required. While solar and wind power already cover a large share of the renewable power production as volatile energy sources, deep geothermal energy offers the specific advantage of providing baseload heat production, especially in winter times when the solar production capacity is reduced. This, as well as the additional potential of using the subsurface for seasonal storage of heat, can make geothermal energy an integral part of solving the challenges of the present and future.

The main obstacles of deep geothermal energy utilisation are the high capital costs and the high exploration risk (World Bank Group 2016). Venture-capital investment is relatively high (up to half of the total investment) until the resource is proven by successful drilling, but profit margins remain low. To attract the attention of potential investors, the exploration risk needs to be minimised by a proper assessment of existing exploration data, quantification of the resulting uncertainties, and subsequent selection of appropriate further exploration measures, resulting in a higher probability of success. Quantifying the uncertainty of key parameters in resource prediction is a contribution to sophisticated decision making regarding minimising the investment risk.

In this study, an approach to quantify the uncertainty of a structural geology within a 3D model is presented, being one of the main tools for resource predictions, drilling target definition, and reservoir modelling. A customised workflow was developed within the modelling software, which allows for the influence of errors of modelling input to be quantified. By quantifying the uncertainty for specific projects, an

*Addresses of the authors:
[1]Technical University of Darmstadt, Institute of Applied Geosciences, Department of Geothermal Science and Technology, Schnittspahnstr. 9, 64287 Darmstadt, Germany
(vandervaart@geo.tu-darmstadt.de / baer@geo.tu-darmstadt.de / frey@geo.tu-darmstadt.de / sass@geo.tu-darmstadt.de)
[2]GeoThermal Engineering GmbH, Baischstr. 8, 76133 Karlsruhe, Germany (Reinecker@Geo-T.de)
[3]Darmstadt Graduate School of Excellence Energy Science and Engineering, Otto-Berndt-Str. 3, 64287 Darmstadt, Germany
[4]Helmholtz-Zentrum Potsdam, Deutsches GeoForschungsZentrum (GFZ), Telegrafenberg, 14473 Potsdam, Germany

DOI: 10.1127/zdgg/2021/0286
E. Schweizerbartsche Verlagsbuchhandlung, Stuttgart, Germany, www.schweizerbart.de

important parameter for the probability of success can be calculated as well, usually the key requirement for exploration insurances covering part of the investor CAPEX in case of failure. An early assessment of uncertainties can reduce the probability of project failure or increase the possibility success by making mitigation efforts such as additional exploration data acquisition (e.g. 2D or 3D seismic, other geophysical exploration methods or exploration wells), project relocation, or upscaling (Witter et al. 2019).

The study presented here is embedded in the framework of the Interreg North-West Europe project DGE-Rollout, which aims to make geothermal energy more accessible. For this project 20 partners from six countries, in particular from Belgium, France, Germany, and the Netherlands, have joined forces to facilitate the use of deep geothermal energy as a climate friendly energy resource to reduce CO_2 emissions and to protect the environment in North-West Europe (Fritschle et al. 2021). Part of this project aims to provide maps that merge the baseline sources in order to identify regional investment hotspots according to the investor profiles. Its limits within structural geological uncertainty, these uncertainties can further be carried into subsequential 3D modelling stages like intrinsic rock property distribution, fracture stimulation prediction, and fluid flow simulations. An early analysis of structural geological uncertainty will give potential investors and stakeholders a head start into unlocking the regional geothermal potential, select further exploration steps, or define early warning criteria for project abandonment.

2. Geological setting

The geothermal potential of the northern Upper Rhine Graben (NURG), i.e. north of Strasbourg, is significant (GeORG Projektteam 2013; Bär et al. 2011). Its tectonic history has resulted in a considerable elevated geothermal gradient of up to 10 K/100 m (Agemar et al. 2012), which is currently exploited by over ten geothermal projects for balneology, home/district/industrial heating, and electrical power generation. Several projects are in development in both the French and German part of the NURG.

The Upper Rhine Graben (URG) extents from Frankfurt (Main) in the north to Basel in the south as a roughly 300 km long and 30 to 40 km broad lowland plain, which is surrounded on all sides by sharply defined mountain ranges. The Rhine River acts as a natural political and administrative boundary of first and second order between Rhineland-Palatinate, Hesse, Baden-Württemberg (Germany), Alsace (France), and Basel (Switzerland).

The URG is part of the European Cenozoic Rift System (Ziegler 1992) extending across Central Europe (Fig. 1). Its tectonic graben structure was formed by rifting processes resulting from Alpine tectonics during the Cenozoic. The graben interior was successively filled by fluvial, lacustrine, and marine sediments up to 4.5 km in overall thickness on top of Permocarboniferous–Mesozoic sediments. Prior to Cenozoic tectonics and sedimentation, the Permocarboniferous–Mesozoic succession was tilted to the south and partly eroded, which has led to the fact that, towards the north, older stratigraphic units are discordantly overlain by Cenozoic sediments.

The Permocarboniferous–Mesozoic strata below the URG rest upon Variscan basement rocks, mainly granitoids and gneisses (Frey et al. 2021). The same basement is exposed at the graben flanks by uplift and erosion (Black Forest, Odenwald, Palatinate, and Vosges mountains). Parts of the Permian strata (i.e. the Rotliegend) correspond to erosional detritus of the former Variscan Orogen, filling intramontane basins and valleys.

The structural geology is characterised by a large number of normal and strike-slip faults oriented roughly parallel to the graben border faults. Dominating geological structures in the study area are ENE–WSW to NW–SE trending normal and strike-slip faults extending from the basement to the Mesozoic and also affecting the Tertiary sequence above.

Crustal thinning and radiogenic heat production in granitic basement rocks define the main heat sources. The thick clay rich Tertiary strata with low thermal conductivity act as a thermal blanket (Freymark et al. 2017), and large crustal and active fault zones host highly permeable fluid pathways enabling heat transport by convection (Freymark et al. 2019), which are the main source of the geothermal and heat flow anomalies causing a local geothermal gradients of up to 10 K/100 m.

The area of this study, located in the northern URG (NURG), which stretches from Worms in the south and to the southeast of Frankfurt (Main) at its most northern point (Fig. 1), encompasses a large basin of roughly 20 kilometres in width from west to east and 50 kilometres length from north to south. According to Arndt et al. (2011) and Bär et al. (2011), the Cenozoic sediments in the northern URG can reach a maximum thickness of about 3.5 km. It consists of syn- and post-tectonic sediments, dating from the Eocene until the Quaternary. In the study area, the Cenozoic sediments of main interest for geothermal utilisation are the Niederrödern Group, the Froidefontaine Subgroup, and the Pechelbronn Group. These groups are medium- to coarse-grained, which provides sufficient permeability and are located within a depth where the temperature is high enough for economic direct heat extraction, with the Pechelbronn Group having the highest potential (Hintze et al. 2018).

The Pechelbronn Group, present in nearly the entire URG, is a syn-rift sedimentary group deposited from the upper Eocene until the lower Oligocene (Derer 2003; Grimm & DSK 2011). It consists of dolomitic marlstones with silt- and sandstones and conglomerates, which are the result of a fluvial-lacustrine sedimentation. Particularly present in the

Fig. 1: Left: Overview of the European Cenozoic rift system. **Right**: Location of the model area within the Upper Rhine Graben (modified from Frey et al. 2021). LRG – Lower Rhine Graben, LG – Limagne Graben, BG – Bresse Graben, URG – Upper Rhine Graben, HG – Hessian Graben, SNB – Saar-Nahe Basin.

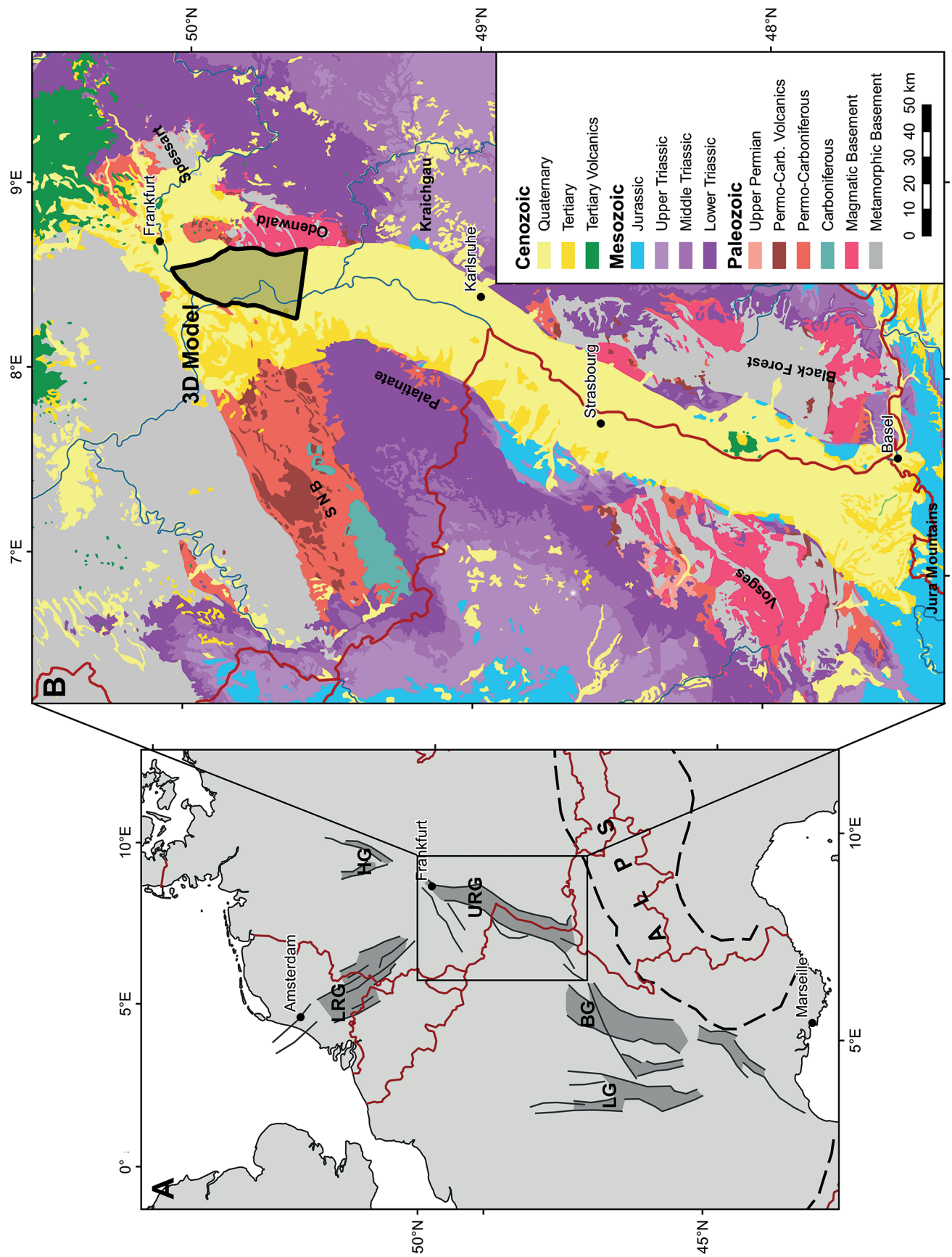
A
B
3D Model
Frankfurt
Amsterdam
Marseille
Karlsruhe
Strasbourg
Basel
Speyer
Odenwald
Kraichgau
Palatinate
SNB
Black Forest
Vosges
Jura Mountains
HG
LRG
URG
BG
LG
S
P
A
0° 5°E 10°E
50°N 45°N
7°E 8°E 9°E
50°N 49°N 48°N
Cenozoic
Quaternary
Tertiary
Tertiary Volcanics
Mesozoic
Jurassic
Upper Triassic
Middle Triassic
Lower Triassic
Paleozoic
Upper Permian
Permo-Carb. Volcanics
Permo-Carboniferous
Carboniferous
Magmatic Basement
Metamorphic Basement
0 10 20 30 40 50 km

Lower and Upper Pechelbronn Formation, these layers can be found to be cut by channel fillings of several metres thickness. In the Middle Pechelbronn Formation, a brackish marine lithology is dominant, characterised by grey marlstones. The entire Pechelbronn Group can be as little as several metres to several hundred of metres thick (GeORG Projektteam 2013).

The sand and marl sequences of the Froidefontaine Subgroup lie directly beneath the Niederrödern Group. In the study area, it can be divided into the Bodenheim Formation (or Rupel Clay Group), the Meletta Group, and the Cyrena Marl Group. The Bodenheim Formation consists of dark clay and marl layers. On top of the Bodenheim Formation is the Meletta Group, represented by clay and marlstones, getting sandier towards the top. Finishing the Froidefontaine Subgroup is the colourful Cyrena Marl Group, with marls and thin fine-grained sandstone layers. This marine-brackish sequence is several hundred metres thick, thinning towards

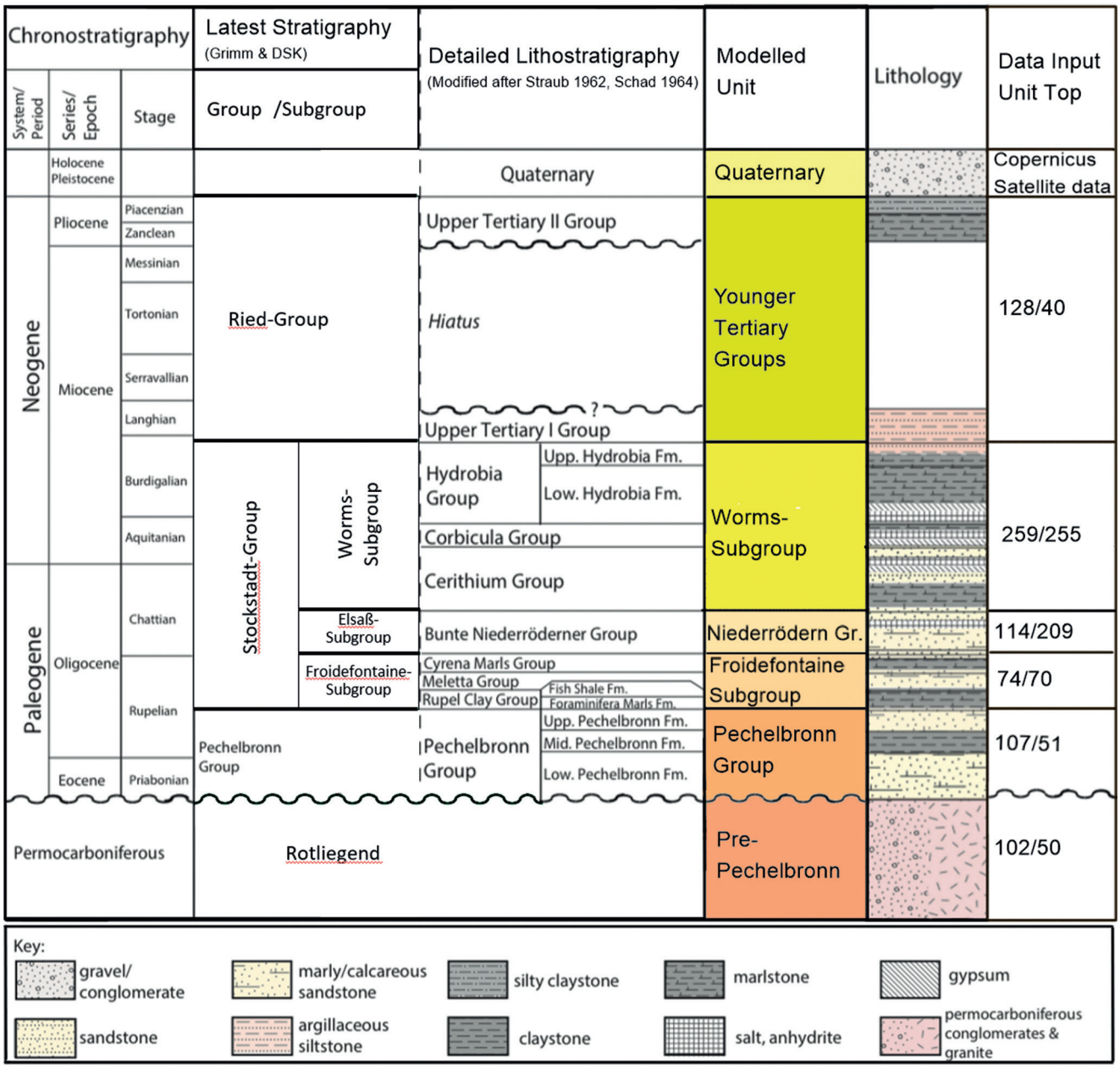

Fig. 2: Lithostratigraphic table of the northern Upper Rhine Graben with an overview of the modelled units in the presented study in comparison to older detailed lithostratigraphic designation (after Straub 1962 and Schad 1964) and the stratigraphic units defined by Grimm (Grimm & Hottenrott 2005) and Grimm & DSK (2011). The last column shows the amount of well markers and the kilometres of 2D seismic lines used for each top horizon. Please note, that the majority of 2D seismic lines and 3D seismic surveys is still not readily available to the public.

100 metres in the north (Maxwell et al. 2016; GeORG Projektteam 2013).

The Niederrödern Group, in the study area overlain by the Worms Group, consists of marls and sandstones. They cover several hundred metres in thickness in the NURG (GeORG Projektteam 2013).

Previous modelling attempts of the Upper Rhine Graben Prior to the model described here, numerous models of the URG have been built to assess its geothermal potential (Arndt et al. 2011; Bär et al. 2011; Koltzer et al. 2019; Freymark et al. 2017; GeORG Projektteam 2013; Bächler et al. 2003; Fig. 2). As main input data for this model, the previous projects "Geopotential of the deep subsurface in the Upper Rhine Graben" (GeORG Projektteam 2013), Hessen 3D (Arndt et al. 2011), and Hessen 3D 2.0 (Bär et al. 2016) have to be specifically mentioned here. These projects provide regional-scale models of parts of the URG and investigate its geothermal potential. While these projects give great insight into the geological structure, the lack of quantified uncertainty mapping limit practical use for engineering purposes. The limitation comes from the lack of quantitative knowledge conveyed in the provided qualitative uncertainty ranges. For example, labelling data with proven, very certain, certain, uncertain, and very uncertain (Arndt et al. 2011) is ambiguous at best, as the meaning of these words are subjective to both author and reader. Without a quantification of the accuracy of the maps and their input data, the validity of the model which laid base to the maps is impossible to determine, making a quantitative uncertainty as an input for potential risk analysis for successful geothermal exploration and exploitation practically impossible.

3. Data and methods

3.1 Data

For this study there was access to 2D seismic profiles and borehole data from various sources such as the Hessisches Landesamt für Naturschutz, Umwelt und Geologie (HLNUG) and the Bundesverband Erdgas, Erdöl und Geoenergie e.V. (BVEG) who represents the data owners. The raw data are supplemented by reports on interpretation attempts. Additionally, the revised and updated interpretation of the large seismic reflection line DEKORP 88'9N (Bär et al. 2021, in prep; Homuth et al. 2021) has been used.

Fault data and interpretations are mainly from the Hessen 3D 2.0 (Bär et al. 2021 and references therein) and the GeORG (GeORG Projektteam 2013) projects. The velocity model used for depth conversion is based on the data compiled from all available seismic lines of Arndt et al. (2011) and Bär et al. (2011).

Finally, interpretation of the basement structure and composition of Frey et al. (2021), based on joint inversion of aeromagnetic and gravimetric data, is adapted.

3.2 Structural modelling

A base model has been created using the input data described above. Well markers, indicating horizons and faults, have been used as interpreted or provided by the HLNUG or BVEG. About 6% of these have been spot checked against available logs. Adaption has been done where needed, due to interpretation errors of location, size, and depth of the faults. These interpretation corrections have then been checked against available seismic lines for verification.

Resolution is chosen by considering input data and the size of the model. A fault grid resolution of 200 metres is selected to achieve acceptable performance. Due to the size of the model, a higher resolution has not achieved any measurable advantage, while disadvantages like running time and project stability decreased. Faults shorter than 2.5 km have been ignored as they have no significant impact on this scale of the model. This is due to the small topological offset they display. Therefore, their uncertainty range is not deemed be sufficient enough to create barriers or pathways that influences within or between units that were not already present in the model. The horizons have a horizontal grid resolution of 100 metres. While this creates a high resolution for a model of this size and therefore a model running time of around 10 minutes, this has little impact on project stability and must be attained for a decent resolution for the uncertainty modelling response desired in this study. For models at exploration permit scale, a higher resolution should be targeted.

3.3 Uncertainty modelling workflow

A customised stochastic approach with multiple realisations has been selected for the uncertainty modelling workflow. While a multitude of different approaches exists in the realm of uncertainty modelling (Wellmann & Caumon 2018), not all are appropriate for the type of information and software used. For instance, sample data uncertainty is limited to input uncertainty only, and does not consider the relationship between data points or interpolation uncertainty. This study uses a probability field technique (Thore et al. 2002) to describe the uncertainties at each location of a horizon, while modelling a complete 3D model similar to approaches described by, for instance, Jessell et al. (2010) and Wellmann et al. (2010). It is based on Monte-Carlo simulations, executing all modelling steps multiple times, yet with different input data. The input data is chosen within the limits of predefined parameters. The predefined parameters define limits of the input data and a distribution function of the values within the limits. Examples of distribution functions are a bell-shaped Gaussian curve, allowing a mean value to have a larger chance of selection, or a uniform distribution indicating all values within the limits have an equal chance of representation. Once a value is selected, it will be used for one run only. When a multitude of models have been created, the maximum modelled uncertainty and standard deviation can be derived from combining the models.

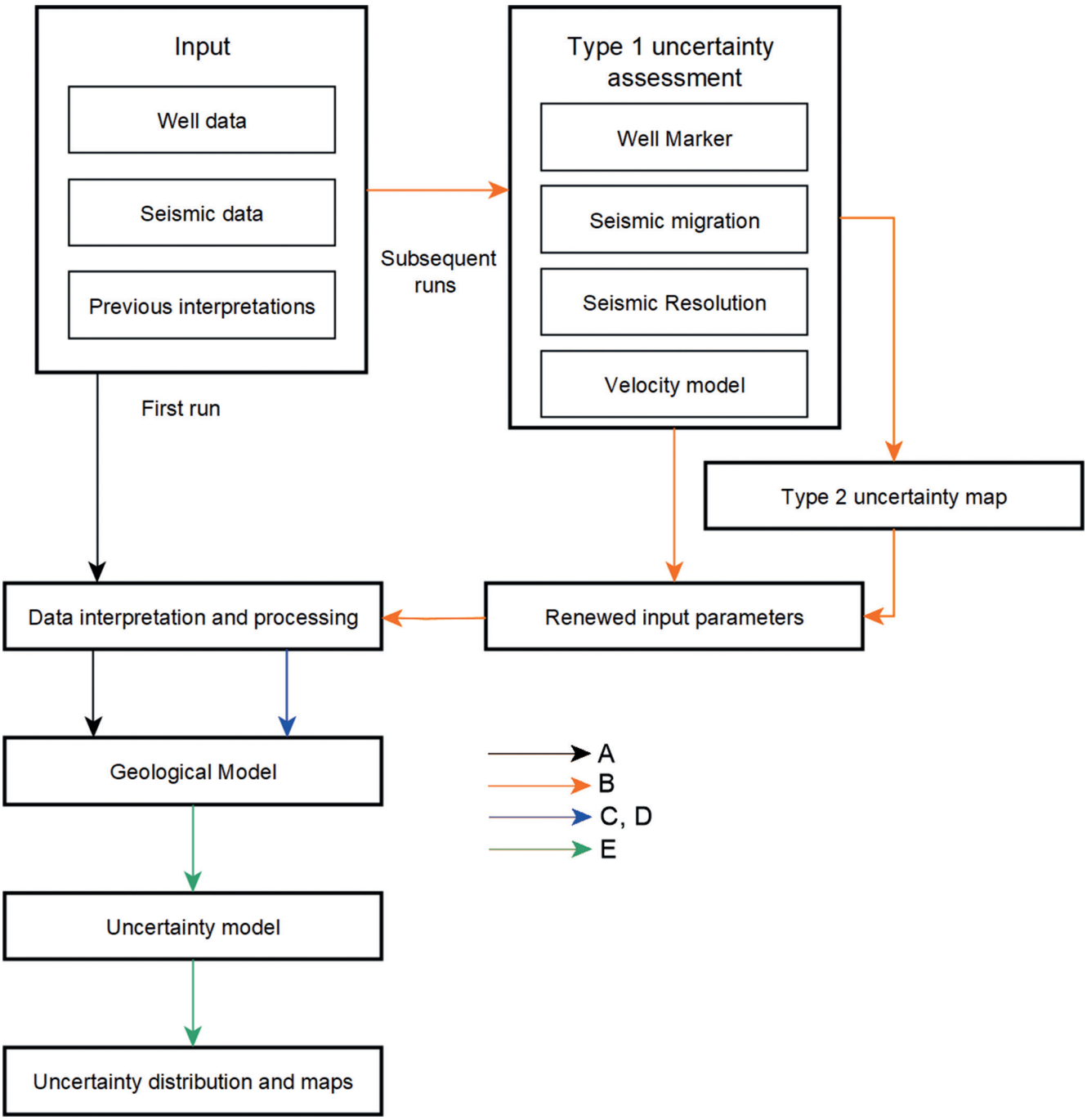

Fig. 3: Overview of the uncertainty modelling workflow.

Schlumberger's Petrel software package (Schlumberger 2020) is used for the workflow that establishes the uncertainty and its impact within the study area. As this does not yet exist within the used software package Petrel 2020, a custom workflow has been developed using its workflow editor and can be used directly in its current native uncertainty modelling workflow, which is solely used for intrinsic rock property and fluid simulation uncertainty modelling. The workflow used here is focussing on the structural uncertainties before rock properties are assigned and consists of several steps:

(A) A base model is created with the best knowledge available to the geomodeller. This creates the workflow and modelling processes the model goes through and is then used as a base case for subsequent uncertainty runs. Inherently, this also fixes the modelling decisions in place like the amount and nature of faults, stratigraphy, and such.

(B) The error ranges of input data are analysed, including their distribution and dependencies. The uncertainty distribution of each error depends on the source data. This can be, but is not limited to, a distribution described by tool manufacturers, benchmark studies, or estimations by scientific studies. The errors and their ranges are subsequently inserted in the developed customised uncertainty modelling workflow.

(C) A representative number of uncertainty models is selected, based on the complexity of the model and amount of uncertainty parameters.

(D) A number, based on (C), of equally probable models are run. Each model uses different input parameters which are randomly selected within the error range of the model (B). Interpolation between data is done using a field, based on a Gaussian random function simulation (GRFS; Gutjahr et al. 1997), which encapsulates the variation between data points.

(E) The new outcomes are analysed and compared. An uncertainty distribution is calculated for each modelled unit, and uncertainty maps are created for visualisation of the uncertainties. This approach has several advantages: (1) Statistically established uncertainty ranges are created, which can be used in any follow-up model; (2) the resulting model gives uncertainty indicators for possible subsequent risk and reward analysis. (3) Variance based sensitivity analysis (Sobol 1993) can be performed to understand the greatest uncertainty components. This information is of service in subsequent decision making for the rest of the process to answer questions about the model. The questions include: (a) how precise the model is, (b) how the uncertainty can be lowered most effectively, and (c) where the most viable location for drilling is (Fig. 3).

3.4 Definition and types of uncertainty

To describe uncertainty, the terms, error, accuracy, and uncertainty itself need to be clearly defined. Accuracy is the closeness of a measured or modelled value to the true value of the object. The error is defined as the difference between a measured or modelled value and the true value of the object. This is different from uncertainty, which can be described as the range of combined measured, observed, theorised, and modelled deviations from the true value of an object. Uncertainty can be grouped in different categories (Mann 1994). This study uses the definition by Wellmann et al. (2010), which separates them in three types: Type 1 (error, bias, and imprecision), Type 2 (stochasticity and inherent randomness), and Type 3 (imprecise knowledge).

Type 1: In any model, input parameters are subject to errors, which are the difference between a reported value and real value, propagating throughout the model (Bardossy & Fodor 2004; Caers 2012). Uncertainty parameters describe the error range of each input component of a model, which typically come from borehole, seismic, and field data. Other uncertainties do exist in the interpretation by geoscientists, such as uncertainty by confirmation bias (Bond 2015). As the latter is not well quantifiable, the former is the focus of this study. The quantifiable input parameters are subject to different types of errors. Errors come mostly from two different technical limitations:

(i) Measurement accuracy and precision, which describe how close the measured value is to the actual value, and how close repetitive measurements are to themselves.

(ii) Resolution, which depends on the measurement device and time/fit for purpose.

As errors are introduced into a model, they propagate within the modelling processes, increasing the total modelled uncertainty.

Type 2: Geological models are subject to a high degree of inter- and extrapolation, where the subsurface rarely displays a linear or smooth relation between input data. Geostatistical methods and processes have been developed to address the uncertainty and relation limitations within modelling (Chilès & Delfiner 2012; Abrahamsen et al. 2012). Due to the large region and syntectonic deposition of the formations, structural relation between data points is only detected within a few kilometres within the model.

Type 3: This type of uncertainty relates to the lack of general knowledge of the modelled area or volume. Sparse data can result in missing significant geological features. These types of uncertainties are difficult to quantify in general and not uncommon, even impossible (Wellmann et al. 2010). In the model, the size and sparsity of source data proves this to be the latter case.

3.5 Quantification of uncertainty for the geothermal field

In this study, our most significant quantifiable uncertainties are of Type 1, sourced from seismic and well data.

Well data: The wells used in the area are mostly nearly vertical. Therefore, only vertical uncertainty as an input for the uncertainty model is considered. Typical sources for vertical uncertainty are elevation reference errors, scaling errors, and stretching and compression. There is no clear consensus on error values in borehole depth uncertainty, as there are different ways of measuring, e.g. measurement while drilling or wireline based. Since well ages are between 5 and 70 years, there is no clear indication for most wells on how depths were measured. Therefore an error value of several metres per kilometre is estimated, based on numbers by Bolt (2019) and Chia et al. (2006) for wells drilled after 1978, when geophysical logging became standard in Hesse. Well markers from wells before 1978, unless indicated otherwise, are considered to have been established by mud logging. These have a significant uncertainty ranging into the tens of metres, which derives from differences in particle discharge and sampling. Particles of different size and density are subject to travelling on a different speed than mud, due to their weight, shape and size, as well as borehole fluid circulation speed and turbulence (Naganawa et al. 2018).

2D seismic: Due to the size of the area, Type 1 and 2 uncertainty is negligible on the horizontal plane. The calcu-

lated uncertainty ranges within tens of metres. Since the modelled horizontal grid is 100 by 100 metres, any horizontal shift of, for instance, faults are not visible. Therefore, only vertical seismic uncertainty components have been considered for modelling. Three seismic processes to define its uncertainty have been used: migration, interpretation error, and depth conversion.

Other uncertainties may be present. However, the quality of the data and the limits to data access does not allow for a more detailed analysis. This is due to regulations and confidentiality agreements within published studies until the beginning of 2021. Other limits are that older data only exist on magnetic tapes and are not digitally available, thus, only low-resolution scanned paper versions of this data have been available. If or when more detailed data becomes available, a more detailed analysis can be made.

The model is comprised of seismic lines of different surveys. As there was no access to the source data, paper scans at correct locations within the model have been used. No check shots were available and petrophysical well log data was limited to a handful of wells. To convert the information picked within the time-model into metric depths, a model of the seismic wave velocities is required. This velocity model was interpolated using the velocity data plotted on the printouts of the seismic lines (Arndt et al. 2011). As exact uncertainty quantification has proven difficult to establish, uncertainty estimation is therefore based on comparing with well point data. Since establishing horizons based on well log data typically has a smaller error than seismic data, as this is a direct measurement instead of an indirect one, a separate model using only point data has been created to establish an approximation depth at the seismic line locations. The residuals between the point-based model and the seismic lines within 500 metres of the well points, provided no fault is present, were interpreted within this range and have been used to calculate the seismic velocity error. This then provides an error, which has subsequently been used as velocity uncertainty component of for the velocity model.

Since only used 2D seismic datasets for this model were accessible, a simplified 2D version of migration uncertainty as proposed by Thore et al. (2002) is used.

$$\Delta X = -2Z\frac{N_x}{N_z}\frac{\Delta V}{V}$$

$$\Delta Z = Z\left(1-\frac{N_x^2}{N_z^2}\right)\frac{\Delta V}{V}$$

where ΔX and ΔZ are uncertainty in horizontal and vertical direction respectively; Z is the depth; $N_{(x,\,z)}$ are the normal vectors at the reflector point; ΔV is the velocity uncertainty; and V is the velocity.

To consider the vertical resolution interpretation error, the interpretation error is constricted to a normal distribution of a quarter wavelength, to allow for the Rayleigh criterion to be taken into account (Kallweit & Wood 1982). In most cases, the reflectors are clear and previous seismic interpretations are shown to be accurate.

Table 1: 2D variogram formation top values using spherical.

	Direction	Minor range (m)	Major range (m)
Niederrödern Group	45	1,050	1,200
Froidefontaine Subgroup	10	1,250	1,400
Pechelbronn Group	37	1,400	1,600

To represent the Type 2 error, interpolation and extrapolation, randomised uncertainty maps have been created for each modelled unit and for each uncertainty run, using a GRFS with both seismic and well tops as input points. These points also form the basis for the variogram, which describes the dissimilarity between points with distance and direction (Table 1).

All errors and uncertainties combined have resulted in a workflow that first creates a well top error point set and a combined seismic uncertainty point set for each unit. These point sets have subsequently been combined with the Type 2 error uncertainty maps. This creates an uncertainty input, which is then added to the original base model. A new run of the model creates a new structural model within the parameters of the uncertainty range. To achieve a high level of confidence, this has resulted in 10,000 models, representing a range showing the extend of the uncertainty within the study area.

4. Results

The base case model (Fig. 4) includes 45 faults, most of them trending N–S to NW–SE. They exhibit mostly a significant normal slip, which resulted in offsets of tens to several hundreds of metres. Seven horizons have been modelled; the formations and groups summing up to a thickness of a maximum of 3.6 kilometres and covering over 1,000 km². The area shows a basement dip towards the south, which is also reflected by the thicknesses of the formations, having more depositional space in the graben. Due to the syntectonic history of the graben, these thicknesses significantly vary laterally and even more between fault blocks. This variation increases with depth, making the Pechelbronn Group the most varying modelled horizon.

The 10,000 individual models show different but equally probable outcomes. Fig. 5 shows a visualisation of the uncertainty for the top horizon of the Niederrödern, Froidefontaine, and Pechelbronn (sub)groups in the NURG. A higher uncertainty is identified in darker blue coloured areas, while light green shows areas of the lowest uncertainty for the three main lithostratigraphic (sub)groups. In all three modelled units, a low uncertainty around wells is identified,

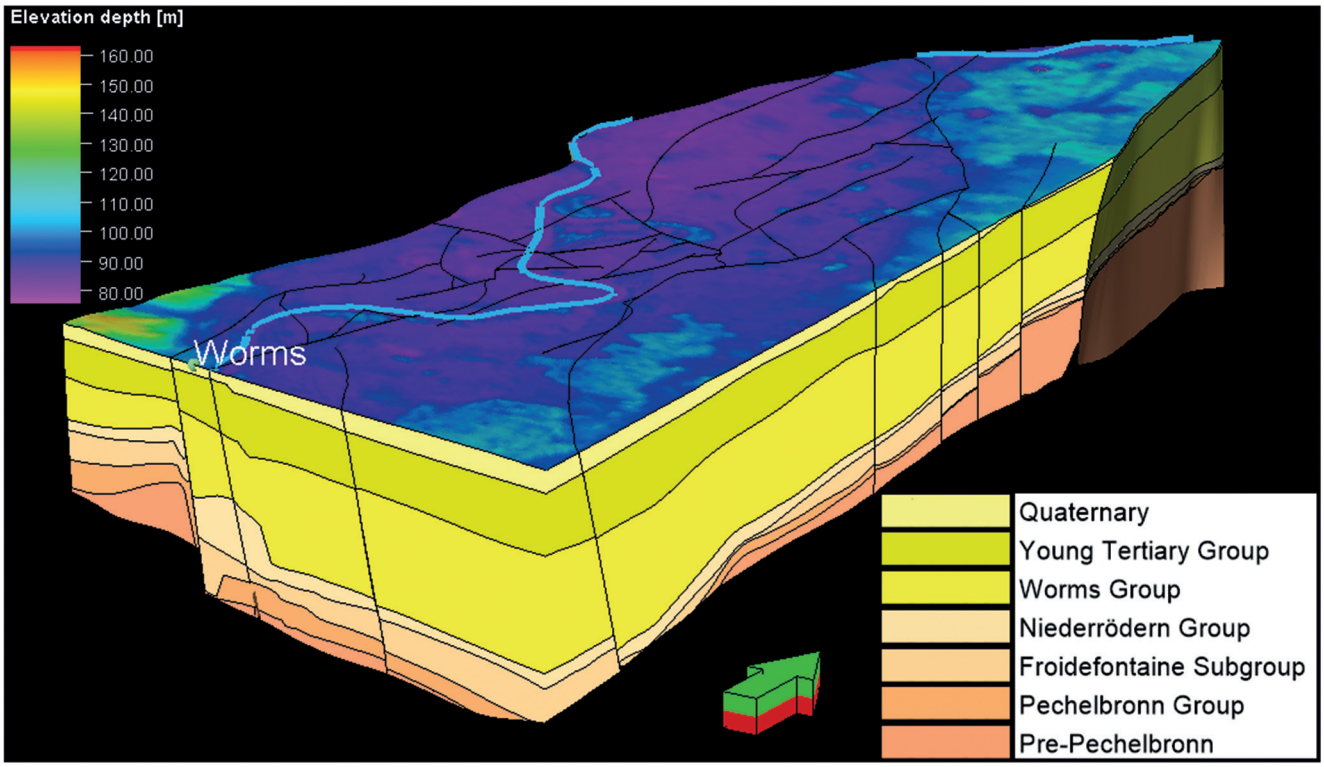

Fig. 4: 3D slice of the base model. Elevation depth signifies the height of the top surface above mean sea level.

whereas seismic exhibits a higher degree of uncertainty. When distance to input increases, uncertainty increases with it. This results in a direct inverse normal distribution relationship between data approximation and uncertainty.

Fig. 6 shows a section of the model from SW to NE, where both well and seismic locations have been indicated. This section shows the influence of wells and seismic lines on the uncertainty range of the modelled (sub)groups. While wells give a very small error of several metres, seismic lines can still give a standard uncertainty of several tens of metres. However, this deviation is greatly reduced with an increase of seismic line density, as depicted on the southwest side of the figure.

A region has been selected to compare the impact of uncertainty reduction by newly added input data, as it would be the case by new seismic lines and exploration wells (Fig. 7). The region of 5 by 5 kilometres, currently has a significant uncertainty with a standard deviation of 92 metres. Two uncertainty models have been created, one with an E–W trending seismic line of 5 km length, the other with a well located in the middle of the area.

5. Discussion

The modelling has shown that with five main uncertainty components, that is well marker depth, seismic migration, seismic interpretation error, velocity model, and modelling interpolation and extrapolation variation, the uncertainty of the model of the NURG ranges to a maximum of over 300 metres in the Pechelbronn Group (Table 2) with a mean standard deviation reaching up to over 70 metres. The results show an increased uncertainty with depth. This is the result of an increase in velocity uncertainty with an increasing two-

Table 2: Overview of uncertainties of the modelled lithological units.

Model Unit	Shallowest top below mean sea level (m)	Deepest top below mean sea level (m)	Mean standard deviation (m)	Minimum standard deviation (m)	Maximum standard deviation (m)
Niederrödern	657	2,788	56.1	1.8	118
Froidefontaine	776	2,958	65.3	2.3	119
Pechelbronn	1,132	3,362	70.0	2.8	129

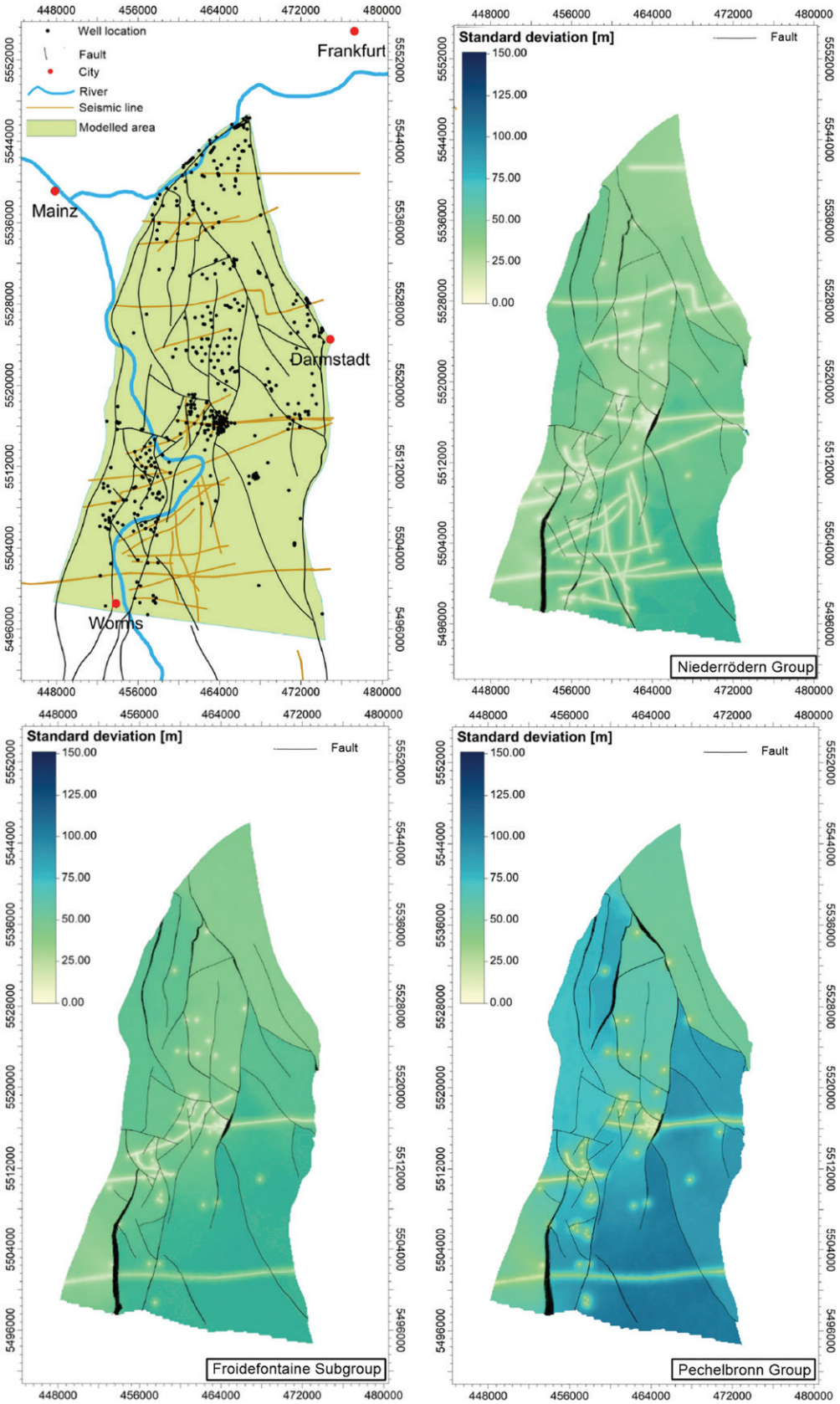

Fig. 5: Overview of the input data used for the model generation and uncertainty (as standard deviation in metres) of the modelled units (or lithostratigraphic (sub)groups).

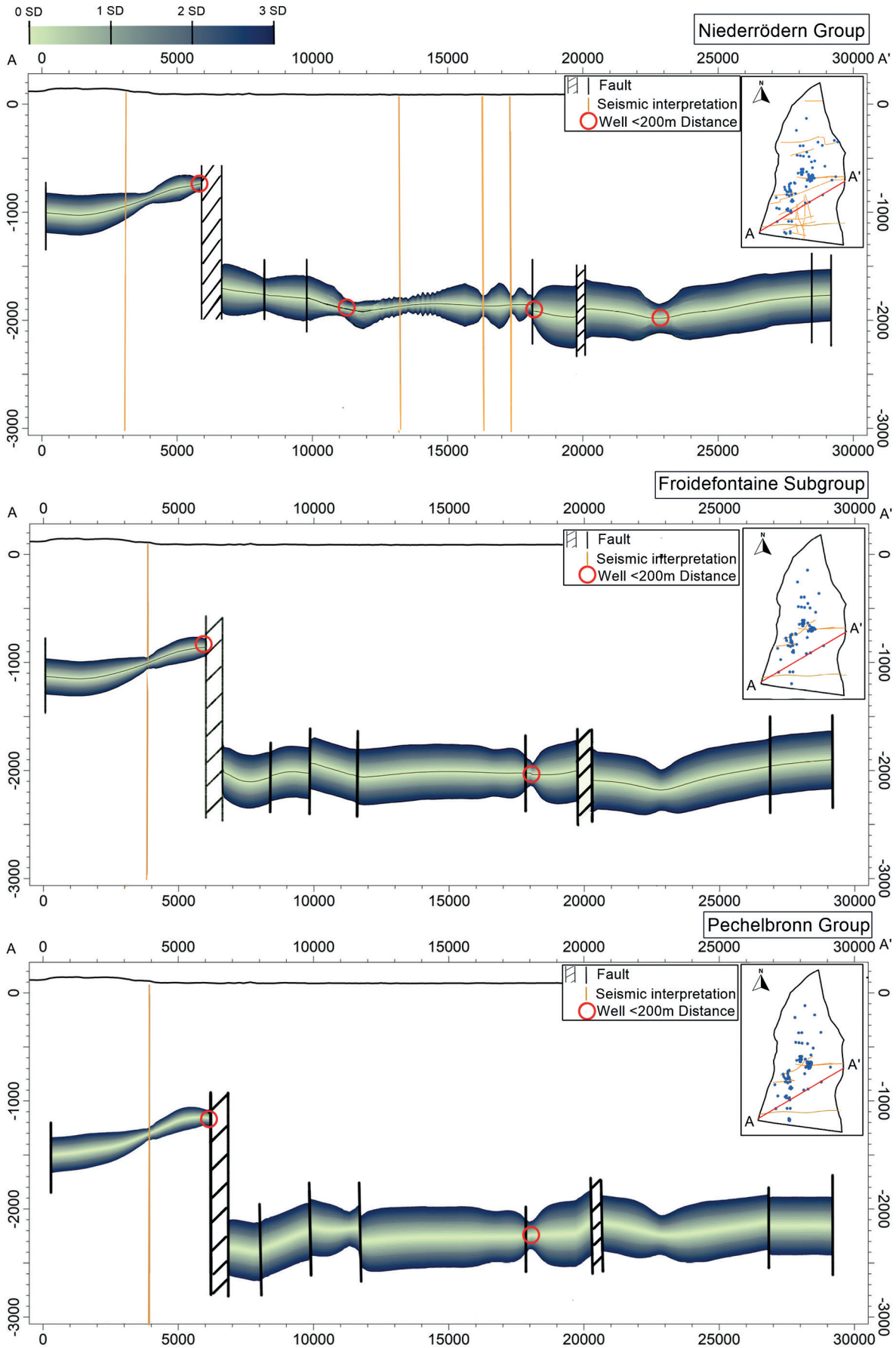
0 SD
1 SD
2 SD
3 SD
Niederrödern Group
Froidefontaine Subgroup
Pechelbronn Group
A
A'
Fault
Seismic interpretation
Well <200m Distance
N
0
5000
10000
15000
20000
25000
30000
-1000
-2000
-3000

Fig. 6: Section SSW–NNE representing uncertainty (given as 0 to 3 standard deviations) for the Niederrödern Group, Froidefontaine Subgroup and Pechelbronn Group. Faults and wells are only represented vertically as they indicate fault or well position at the horizon level. Wells in the vicinity of the profile are only displayed if they have a normal distance to the profile of less than 200 m.

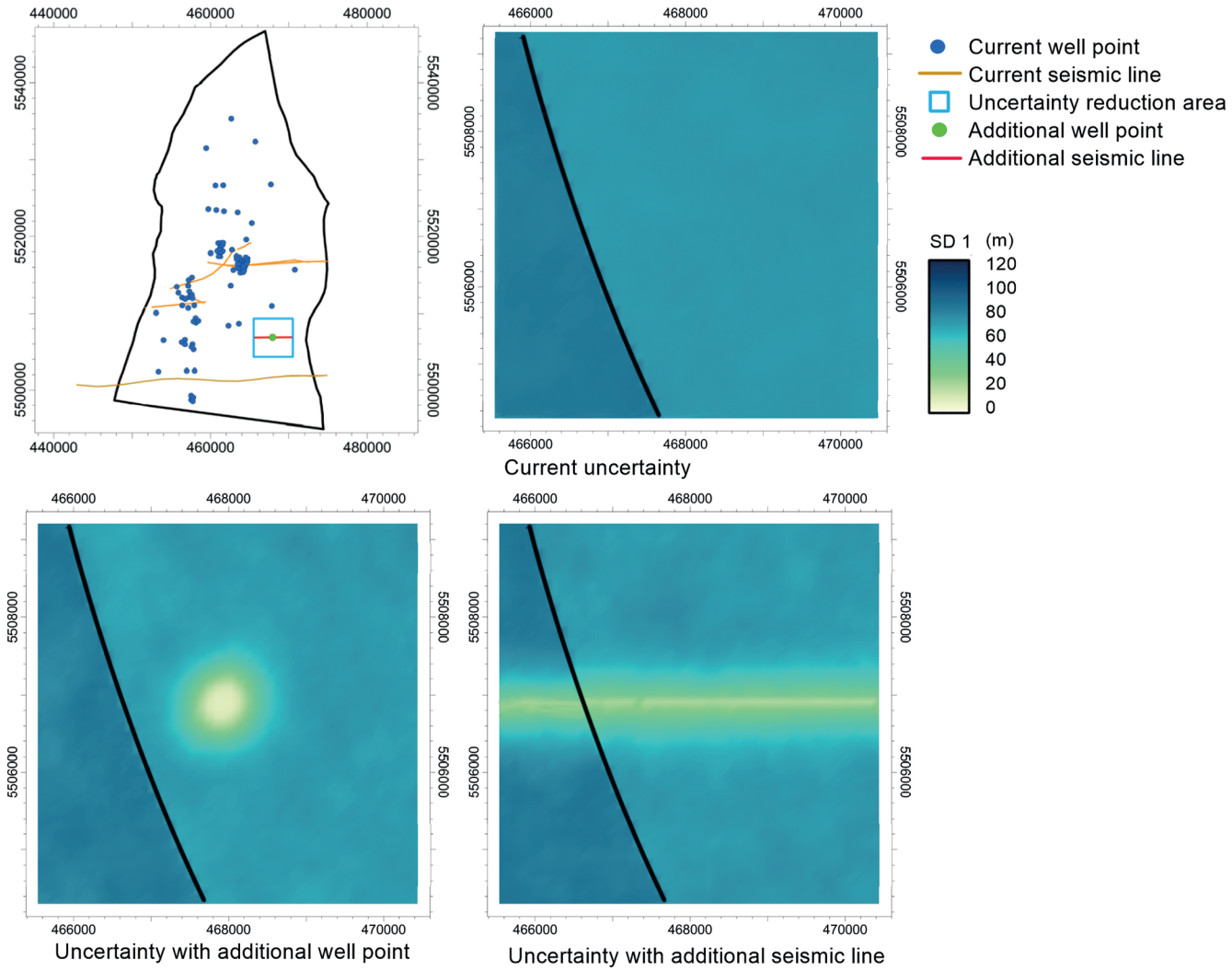

Fig. 7: Representation of uncertainty reduction at the Pechelbronn Group in the indicated area (top left).

way travel time and decreasing well marker data due to the individual borehole depth.

When considering the Type 1 uncertainty, which is mainly dependent on input data errors due to measurements and subsequent formulas, well markers are the component with the least error, significantly decreasing the uncertainty at and near the well location. However, since a well marker is a 1D component, the influence of a single point is only of limited importance for the entire regional model.

While compared to well top data, seismic is less accurate and does have the advantages of being a considerably cheaper and less invasive method, giving a broader spatial view than an exploration or test well can provide. Perner (2018) reports that 3D seismic surveys in the area by non-public sources have an offset maximum of 30 metres, compared to well point data. In addition to what is presented in this publication, a model with these parameters indicates a reduction of the standard deviation of the Pechelbronn Group within the study area by 58 % in total and by even 63 to 87 % for the area which is directly covered by the 3D seismic survey.

Another important point is that well data can reduce seismic uncertainty significantly. Indeed, a significant accuracy of seismic and well depth can be achieved with a seismic well tie, using vertical seismic profiles (VSP) or a synthetic VSP (Hardage 1985).

Uncertainty is highest where input data is sparse, which results in the uncertainty to be more driven by Type 2 uncer-

tainty. To reduce the uncertainty, several solutions are possible:

(1) Increasing the geological understanding: lowering the variability limits of the interpolation and extrapolation algorithm.

(2) Reassessing available data and, if needed, acquiring new data. Ideally as low-cost solution, firstly, more of the vintage data could be digitised, which has not been fully accessible for the model presented here, due to the reasons described above. Remaining areas with data sparsity can then be the target of additional exploration campaigns, including 2D seismic, 3D seismic, and other geophysical surveys, as well as exploration wells with new petrophysical logging. Additional surveys, be it seismic, aeromagnetic, or otherwise, could also indicate faults where presently no data has used for interpretation.

Theoretical data acquisition impact

An investigation of the impact for such a decision has been made by creating models with an additional seismic line or well (Fig. 7, Table 3). This shows a clear reduction of structural model uncertainty by acquiring new exploration data. Seismic has a smaller remaining uncertainty and the costs per study area are expected to be lower. Another advantage is the less invasive nature of the method, which reduces local population resistance. It must be noted, that even though a well is more expensive, well logging has other advantages with geophysical methods and already provides input for reservoir characterisation in much greater detail, which further reduced prospective risks. The different geophysical logs and additional well testing methods can provide indications of, for instance, temperature, permeability, porosity, in situ stress, fracture network, fluid composition, and other intrinsic properties. Another point is that drilling a well is a smaller operation in terms of area, while a 5 km seismic line needs an up to 10 km long acquisition for a very clear result

What is not present in the model are structural anomalies, such as faults, that are undetected or unpublished and thus far from public domain. While these Type 3 uncertainties are present, as there is no indication of their locations or likelihood, it remains impossible to quantify these. From several 2D seismic lines it is known that more faults are present, but data sparsity prevents either to quantify their size or trace their horizontal extent and orientation. Therefore, while undetected independent fault blocks may be present, they cannot be presented or assessed by the current uncertainty model.

In summary, several models have been created on the topology and geometry of lithostratigraphic units of the NURG, which provide a good starting point for further deep geothermal exploration. However, due to uncertainties provided by data errors and coverage, these models could significantly lack accuracy. This could be reduced by re-evaluation of the source data and additional data acquisition. Furthermore, it goes in hand with findings of Reinhold et al. (2016), which addresses the benefits of 3D surveys in the URG, significantly reducing unquantifiable Type 3 uncertainties, which especially delineate the geometries of fault zones and are often the main target of deep geothermal exploitation due to their increased permeability.

While different uncertainty analysis methods are possible (Bardossy & Fodor 2004), many are impractical due to their inherent limitations or limitations with current modelling software. Stochastic uncertainty analysis is intuitive and are present in many software. The structural uncertainty analysis workflow, established and written for this study, can be used seamlessly with further steps within a complete modelling and uncertainty workflow.

6. Conclusion

Uncertainty modelling has provided valuable additional information on the depth and thickness of potential geothermal reservoir units of the NURG and helped to identify areas where additional exploration data is required to properly reduce exploration risks. Between well data and seismic, the latter is the greatest contributor of uncertainty. However, while well markers have a smaller error, they provide less information on the model scale, which hides structures that seismic exploration campaigns are able to clearly expose.

This study shows that uncertainty analysis is essential for providing guidance to uncertainty reduction measures in the form of acquiring new exploration data. In the NURG, significant uncertainty is present, reaching standard deviations

Table 3: Uncertainty reduction corresponding with the area indicated in Fig. 7. (1) Assuming a 10 km long seismic line in E–W direction, for sufficient correlation with other subsurface data. Estimated costs (100 k€) include acquisition and processing, but without costs for approval procedure, planning, tendering, permitting, mobilisation, and interpretation. (2) Assumed drilling cost (2,300 k€/km) until top depth, including logging.

	Well top depth	Current mean uncertainty (m)	Mean uncertainty with added 2D seismic survey (m)	Mean uncertainty with added exploration well (m)	Estimated costs seismic survey in k€ (1)	Estimated costs well drilling in k€ (2)
Niederrödern Group	2,044	80.8	71.1	76	100	4,701
Froidefontaine Subgroup	2,287	90.8	81.1	86	100	5,260
Pechelbronn Group	2,350	93.0	85	89.4	100	5,405

of hundreds of metres in deeper strata and in regions with scarce data availability. By analysing the structural modelling uncertainty, the reliability of models is quantified. Reduction of these uncertainties can be addressed by additional data acquisition or an increased variability study within the formation. It also indicates which areas are in need of further uncertainty reduction, thus efforts to increase model accuracy can be focussed.

In a broader view, proper uncertainty modelling provides a quick and cheap method to further improve geological subsurface models. It can also provide an insight for future projects to decide which course of uncertainty reductions is most effective. It is therefore imperative to set aside time to evaluate the uncertainty in order to increase project success and profitability.

This study only outlines the uncertainty of structural geology and its model. However, for a complete geothermal resource assessment, intrinsic and intensive properties and their uncertainties need to be modelled. To name a few, permeability and reservoir temperature are of utmost importance, yet other petrophysical properties like porosity, thermal conductivity, heat capacity, and radiogenic heat production are also necessary for predicting the thermo-hydraulic behaviour of the reservoirs and thus be able to assess their economic potential. This remains for future studies. Yet, before these properties can be modelled, the formations' limits and thicknesses need to be properly outlined first, and their uncertainties be mapped as in the scope of this study.

7. Acknowledgements

This study would not have been possible without the Petrel licences, kindly provided by Schlumberger. Furthermore, both the HLNUG and the BVEG were essential for supplying data. This study was supported by the Interreg NWE Programme through the Roll-out of Deep Geothermal Energy in North-West Europe (DGE-ROLLOUT) Project (www.nweurope.eu/DGE-ROLLOUT). The Interreg NWE Programme is part of the European Cohesion Policy and financed by the European Regional Development Funds (ERDF).

8. References

Abrahamsen, P., Hauge, R., & Kolbjørnsen, O. (2012). *Geostatistics Oslo 2012*. Dordrecht: Springer. https://doi.org/10.1007/978-94-007-4153-9

Agemar, T., Schellschmidt, R., & Schulz, R. (2012). Subsurface temperature distribution in Germany. *Geothermics, 44*, 65–77. https://doi.org/10.1016/j.geothermics.2012.07.002

Arndt, D., Bär, K., Fritsche, J.-G., Kracht, M., Sass, I., & Hoppe, A. (2011). 3D structural model of the Federal State of Hesse (Germany) for geopotential evaluation. *Zeitschrift der Deutschen Gesellschaft für Geowissenschaften, 162*(4), 353–369. https://doi.org/10.1127/1860-1804/2011/0162-0353

Bächler, D., Kohl, T., & Rybach, L. (2003). Impact of graben-parallel faults on hydrothermal convection – Rhine Graben case study. *Physics and Chemistry of the Earth, A/B/C 28*(9–11), 431–441. https://doi.org/10.1016/S1474-7065(03)00063-9

Bär, K., Arndt, D., Fritsche, J.-G., Götz, A. E., Kracht, M., Hoppe, A., & Sass, I. (2011). 3D-Modellierung der tiefengeothermischen Potenziale von Hessen – Eingangsdaten und Potenzialausweisung. *Zeitschrift der Deutschen Gesellschaft für Geowissenschaften, 162*(4), 371–388. https://doi.org/10.1127/1860-1804/2011/0162-0371

Bär, K., Hintze, M., Weinert, S., Sippel, J., Freymark, J., Scheck-Wenderoth, M., & Sass, I. (2016). Das Verbundprojekt Hessen 3D 2.0. *Geothermische Energie, 85*(3), 24–25.

Bär, K., Homuth, B., Stiller, M., Weinert, S., Bott, J., & Oncken, O. et al. (2021. (in prep)). New interpretation of a reprocessed crustal scale seismic profile across the Mid German Crystalline High and the Northern Upper Rhine Graben, Germany. *Geochemistry Geophysics Geosystems*.

Bardossy, G., & Fodor, J. (2004). *Evaluation of uncertainties and risks in geology. New mathematical approaches for their handling*. Berlin: Springer. https://doi.org/10.1007/978-3-662-07138-0

Bolt, H. (2019). Increasing value through reducing differences between LWD and wireline depths. In *SPE Annual Technical Conference and Exhibition. Calgary, Alberta, Canada*, 2019-09-23. https://doi.org/10.2118/196035-MS

Bond, C. E. (2015). Uncertainty in structural interpretation: Lessons to be learnt. *Journal of Structural Geology, 74*, 185–200. https://doi.org/10.1016/j.jsg.2015.03.003

Caers, J. (2012). *Modeling uncertainty in the earth sciences*. Hoboken: Wiley.

Chia, C., Laastad, H., Kostin, A., Hjortland, F., & Bordakov, G. (2006). A new method for improving LWD logging depth. In *Proceedings of SPE Annual Technical Conference and Exhibition*, 24–27/09/2006. https://doi.org/10.2118/102175-MS

Chilès, J.-P., & Delfiner, P. (2012). *Geostatistics. Modeling spatial uncertainty*. Hoboken: Wiley. https://doi.org/10.1002/9781118136188

Derer, C. E. (2003). Tectono-sedimentary evolution of the northern Upper Rhine Graben (Germany), with special regard to the early syn-rift stage. *Dissertation University of Bonn* (103 pp.).

Frey, M., Weinert, S., Bär, K., van der Vaart, J., Dezayes, C., Calcagno, P., & Sass, I. (2021). Integrated 3D geological modelling of the northern Upper Rhine Graben by joint inversion of gravimetry and magnetic data. *Tectonophysics, 813*, 228927. https://doi.org/10.1016/j.tecto.2021.228927

Freymark, J., Sippel, J., Scheck-Wenderoth, M., Bär, K., Stiller, M., Fritsche, J.-G., & Kracht, M. (2017). The deep thermal field of the Upper Rhine Graben. *Tectonophysics, 694*, 114–129. https://doi.org/10.1016/j.tecto.2016.11.013

Freymark, J., Bott, J., Cacace, M., Ziegler, M., & Scheck-Wenderoth, M. (2019). Influence of the main border faults on the 3D hydraulic field of the central Upper Rhine Graben. *Geofluids, 2019*, 1–21. https://doi.org/10.1155/2019/7520714

Fritschle, T., Petitclerc, E., van Melle, T., Broothaers, M., Passamonti, A., Arndt, M., … & Salamon, M. (2021). DGE-ROLLOUT: Promoting Deep Geothermal Energy in North-West Europe. *Proceedings World Geothermal Congress*, 2021, *Reykjavik*.

GeORG Projektteam (2013). Geopotenziale des tieferen Untergrundes im Oberrheingraben. *Fachlich-Technischer Abschlussbericht des Interreg-Projekts GeORG*. http://www.geopotenziale.eu

Grimm, K. I., & DSK – Deutsche Stratigraphische Kommission (Eds.) (2011). Stratigraphie von Deutschland, IX. Tertiär, Teil

1: Oberrheingraben und benachbarte Tertiärgebiete. *Schriftenreihe der Deutschen Gesellschaft für Geowissenschaften, 75*, 1–461.

Grimm, M. C., & Hottenrott, M. (2005). Das Tertiär des Oberrheingrabens in der Stratigraphischen Tabelle von Deutschland 2002. *Newsletters on Stratigraphy, 41*(1–3), 351–358. https://doi.org/10.1127/0078-0421/2005/0041-0351

Gutjahr, A., Bullard, B., & Hatch, S. (1997). General joint conditional simulations using a fast fourier transform method. *Mathematical Geology, 29*(3), 361–389. https://doi.org/10.1007/BF02769641

Hardage, B. A. (1985). *Vertical seismic profiling. Part A: Principles* (2nd ed.). London: Geophysical Press.

Hintze, M., Plasse, B., Bär, K., & Sass, I. (2018). Preliminary studies for an integrated assessment of the hydrothermal potential of the Pechelbronn Group in the northern Upper Rhine Graben. *Advances in Geosciences, 45*, 251–258. https://doi.org/10.5194/adgeo-45-251-2018

Homuth, B., Bär, K., Weinert, S., & Stiller, M. (2021). Reprocessing of the Hessian DEKORP seismic profiles. *Conference Paper, Jahrestagung der Deutschen Geophysikalischen Gesellschaft*. https://doi.org/10.23689/fidgeo-3945

Jessell, M. W., Ailleres, L., & de Kemp, E. A. (2010). Towards an integrated inversion of geoscientific data: What price of geology? *Tectonophysics, 490*(3–4), 294–306. https://doi.org/10.1016/j.tecto.2010.05.020

Kallweit, R. S., & Wood, L. C. (1982). The limits of resolution of zero-phase wavelets. *Geophysics, 47*(7), 1035–1046. https://doi.org/10.1190/1.1441367

Koltzer, N., Scheck-Wenderoth, M., Cacace, M., Frick, M., & Bott, J. (2019). Regional hydraulic model of the Upper Rhine Graben. *Advances in Geosciences, 49*, 197–206. https://doi.org/10.5194/adgeo-49-197-2019

Mann, J. C. (1994). Uncertainty in geology. In J. C. Davis & U. C. Herzfeld (Eds.), *Computers in Geology – 25 years of progress* (pp. 241–254). Oxford: Oxford University Press. https://doi.org/10.1093/oso/9780195085938.003.0025

Maxwell, E. E., Alexander, S., Bechly, G., Eck, K., Frey, E., Grimm, K., . . . Ziegler, R. (2016). The Rauenberg fossil Lagerstätte (Baden-Württemberg, Germany): A window into early Oligocene marine and coastal ecosystems of Central Europe. *Palaeogeography, Palaeoclimatology, Palaeoecology, 463*, 238–260. https://doi.org/10.1016/j.palaeo.2016.10.002

Naganawa, S., Suzuki, M., Ikeda, K., Inada, N., & Sato, R. (2018). Modeling of cuttings lag distribution in directional drilling to evaluate depth resolution of mud logging. In *IADC/SPE Drilling Conference and Exhibition, Fort Worth, Texas, USA, 2018-03-06*. https://doi.org/10.2118/189615-MS

Perner, M. (2018). Evolution of palaeoenvironment, kerogen composition and thermal history in the Cenozoic of the Northern Upper Rhine Graben, SW-Germany. *Dissertation University of Heidelberg* (222 pp.). https://doi.org/10.11588/heidok.00024385

Reinhold, C., Schwarz, M., Bruss, D., Heesbeen, B., Perner, M., & Suana, M. (2016). The northern Upper Rhine Graben: Re-dawn of a mature petroleum province? *Swiss Bulletin für Angewandte Geologie, 21*(2), 35–56. https://doi.org/10.5169/seals-658196

Schlumberger (2020). *Petrel. Seismic to simulation. Version 2020.2.*

Schad, A. (1964). Feingliederung des Miozäns und die Deutung der nacholigozänen Bewegungen im Mittleren Rheingraben. *Abhandlungen des Geologischen Landesamtes Baden-Württemberg, 5*, 1–56.

Sobol, I. M. (1993). Sensitivity estimates for nonlinear mathematical models. *Mathematical Modelling and Computational Experiments, 1*(4), 407–414.

Straub, E. W. (1962). Die Erdöl- und Erdgaslagerstätten in Hessen und Rheinhessen. *Abhandlungen des Geologischen Landesamtes Baden-Württemberg, 4*, 123–136.

Thore, P., Shtuka, A., Lecour, M., Ait-Ettajer, T., & Cognot, R. (2002). Structural uncertainties: Determination, management, and applications. *Geophysics, 67*(3), 840–852. https://doi.org/10.1190/1.1484528

Wellmann, F., & Caumon, G. (2018). 3-D structural geological models: Concepts, methods, and uncertainties. *Advances in Geophysics, 59*, 1–121. https://doi.org/10.1016/bs.agph.2018.09.001

Wellmann, F., Horowitz, F. G., Schill, E., & Regenauer-Lieb, K. (2010). Towards incorporating uncertainty of structural data in 3D geological inversion. *Tectonophysics, 490*(3–4), 141–151. https://doi.org/10.1016/j.tecto.2010.04.022

Witter, J. B., Trainor-Guitton, W. J., & Siler, D. L. (2019). Uncertainty and risk evaluation during the exploration stage of geothermal development: A review. *Geothermics, 78*, 233–242. https://doi.org/10.1016/j.geothermics.2018.12.011

World Bank Group (2016). Comparative analysis of approaches to geothermal resource risk mitigation: A global survey. *ESMAP Knowledge Series, 024*(16), 1–35. https://openknowledge.worldbank.org/handle/10986/24277

Ziegler, P. A. (1992). European Cenozoic rift system. *Tectonophysics, 208*(1–3), 91–111. https://doi.org/10.1016/0040-1951(92)90338-7

Manuscript received: 08.03.2021
Revisions required: 07.05.2021
Revised version received: 09.07.2021
Accepted for publication: 08.10.2021